# Proteomic profiling reveals a severely perturbed protein expression pattern in aged skeletal muscle

KATHLEEN O'CONNELL,  JOAN GANNON,  PHILIP DORAN  and  KAY OHLENDIECK

Department of Biology, National University of Ireland, Maynooth, Co. Kildare, Ireland

**Abstract.** Extended longevity is often accompanied by frailty and increased susceptibility to a variety of crippling disorders. One of the most striking features of human aging is sarcopenia, which is defined as the age-related decline in skeletal muscle mass and strength. Although various metabolic and functional defects in aging muscle fibres have been described over the last decade, it is not known whether a pathophysiological hierarchy exists within degenerative pathways leading to muscle wasting. Hence, in order to identify novel biomarkers of age-dependent skeletal muscle degeneration, we have here applied mass spectrometry-based proteomics for studying global muscle protein expression patterns. As a model system of sarcopenia, we have employed crude extracts from senescent rat *gastrocnemius* muscle, as compared to young adult tissue preparations. Using the highly sensitive protein dye Deep Purple for the analysis of the 2-D separated muscle proteome and peptide mass fingerprinting for the identification of individual protein spots, a differential expression pattern was observed for contractile proteins, metabolic factors, regulatory components and heat shock elements. A drastic increase was shown for αB-crystallin, myosin light chain MLC-1, phospho-glycerate kinase, adenylate kinase, triosephosphate isomerase, albumin, aconitase and nucleoside-diphosphate kinase in aged fibres. In contrast, the expression of pyruvate kinase, aldolase, creatine kinase, transferrin, α-tropomyosin and myosin light chain MLC-3 was decreased in old skeletal muscle. Comparative 2-D immunoblotting of selected candidate proteins has confirmed the effect of aging on the skeletal muscle proteome. These findings demonstrate a severely perturbed protein expression pattern in aged skeletal muscle, which reflects the underlying molecular alterations causing a drastic decline of muscle strength in the senescent organism. In the long-term, the systematic deduction of abnormal protein expression in aged muscle by proteomic profiling approaches may lead to the cataloguing of a cohort of novel therapeutic targets to treat muscular weakness in the aging population.

---

*Correspondence to:* Professor Kay Ohlendieck, Department of Biology, National University of Ireland, Maynooth, Co. Kildare, Ireland
E-mail: kay.ohlendieck@nuim.ie

## Introduction

During aging, cellular alterations in the capacity to maintain normal homeostasis play a central role in the reduced biological function of many tissue and organ systems. The senescent organism is predisposed to a host of pathologies including cardiovascular disorders, cancer and neurodegenerative diseases. Sarcopenia, the age-related decline in skeletal muscle mass and strength, is another major complication in the elderly (1-3). Since senescent muscle wasting is not well understood on the molecular and cellular level, no effective treatment has yet been developed to counteract age-related fibre degeneration (4-6). A variety of pathogenic mechanisms are currently being discussed that might be involved in rendering muscles more susceptible to fiber atrophy (7). Since skeletal muscle represents the most abundant tissue in the body, fiber degeneration has severe consequences for movement, posture, the overall integration of metabolism and heat homeostasis (8).

Age-dependent muscle weakness is associated with oxidative stress, impaired mitochondrial metabolism, decreased microcirculation, increased apoptosis, altered post-translational modifications of key muscle proteins, free radical production, changed hormonal responses, a decreased regenerative potential and impaired neuronal signal transduction (9-15). The proposed molecular basis for abnormal triad signaling in aged fibres is a drastic reduction in voltage-sensing $\alpha_{1S}$-dihydropyridine receptor units at the transverse tubules, leading to excitation-contraction uncoupling (16). This triggers a pathophysiological increase in the percentage of sarcoplasmic reticulum $Ca^{2+}$-release channels that are not physically coupled to the voltage-sensor (17). The consequence is abnormal $Ca^{2+}$-handling and impaired initiation of contraction. In addition, denervation of aged fibres may represent a key pathological insult to the motor unit system resulting in muscular atrophy (18,19).

Since muscle degeneration is characteristic of the aging process in humans, this warrants a detailed biochemical analysis into the differential protein expression pattern between young and old fibres. Proteomics, the large-scale and high-throughput biochemical approach to study entire protein

complements (20), suggests itself for the global identification of complex alterations in aged tissues (21). The systematic deduction of altered protein expression patterns during the aging process may lead to the discovery of new therapeutic targets to counteract sarcopenia of old age (22). Mass spectrometric peptide mass fingerprinting is an ideal biochemical identification tool for the swift cataloguing of muscle proteins involved in fibre degeneration, as recently reviewed by Doran *et al* (23) and has been applied in this study.

Over the last few decades of biomedical research, both spontaneous and genetically engineered animal models of muscular disorders have been employed for investigating pathophysiological processes. Skeletal muscle specimens from inbred animal strains exhibit genetically much less inter-individual differences as compared to patient biopsies, therefore considerably lower experimental repeats can be used in initial proteomic profiling exercises. Based on the findings from comparative animal model analyses, a more informed decision on the design of clinical studies could be reached (24). Hence, cohorts of new biomarkers identified by animal model proteomics can then be used for an in-depth characterization of diseased human muscles in order to improve diagnostic procedures or design better treatment strategies.

30-month old Wister rats represent an established animal model of skeletal muscle aging. A variety of studies have been performed with this inbred animal strain (16,25-27). Since a previous proteomic study, which focused on 7 versus 18 versus 30-month old rats, demonstrated that 7-month old muscle and 18-month old muscle exhibited similar protein expression pattern (27), we have carried out here a comparative profiling of young adult (3-months) versus senescent (30-months) skeletal muscle fibres. In contrast to the 2-D gel electrophoretic analysis based on Coomassie Brilliant Blue R-250 by Piec *et al* (27), we have here employed the more sensitive fluorescent protein dye Deep Purple for the staining of differentially expressed muscle proteins. Epicoccone, the active ingredient in Deep Purple total protein stain, is a novel fluorescent compound from the fungus *Epicoccum nigrum* (28,29) which is a superior protein dye as compared to non-fluorescent probes (30). The proteomic profiling of aged skeletal muscle fibres revealed a differential expression pattern for metabolic enzymes, contractile elements, stress proteins and regulatory components. These findings demonstrate that a severely perturbed protein expression pattern is associated with the drastic decline of muscle mass and strength in the senescent organism.

## Materials and methods

*Materials*. Electrophoresis grade chemicals, the 2-D Quant kit for protein quantification, 24-cm IPG strips (pH 3.0-10), IPG ampholytes (pH 3.0-10), fluorescent protein dye Deep Purple stock solution and acetonitrile were purchased from Amersham Biosciences/GE Healthcare (Little Chalfont, Bucks., UK). Protease inhibitors were from Roche Diagnostics (Mannheim, Germany). Ultrapure Protogel acrylamide stock solutions were from National Diagnostics (Atlanta, GA, USA). DNase-I enzyme was from Sigma Chemical Co. (Dorset, UK). A matrix kit containing α-cyano-4-hydroxycinnamic acid and an external calibration peptide mixture was obtained from

Laserbiolabs, Sophia-Antipolis, France. Sequencing grade-modified trypsin was purchased from Promega (Madison, WI, USA). Chemiluminescence substrate was from Pierce and Warriner (Chester, UK) and nitrocellulose membranes were purchased from Millipore (Bedford, MA, USA). All other chemicals were of analytical grade and purchased from Sigma Chemical Co.

*Antibodies*. Primary antibodies that recognize skeletal muscle markers were from Abcam Ltd., Cambridge, UK (pAb ab6910 to muscle aldolase, pAb ab28760 to triosephosphate isomerase, pAb ab9033 to transferrin); Abgent, San Diego, CA, USA (pAb AP7094b to phosphoglycerate kinase 1, pAb ap1936c to aconitase isoform ACO2); Abnova GmbH, Heidelberg, Germany (mAb A412-1A3 to the muscle-specific CA3-isoform of carbonic anhydrase); and Santa Cruz Biotechnology, Santa Cruz, CA, USA (pAb sc-28785 to adenylate kinase isoform AK1). Peroxidase conjugated secondary antibodies were purchased from Chemicon International (Temecula, CA, USA).

*Extraction of total muscle protein complement*. As an established animal model of sarcopenia, the *gastrocnemius* muscle from 30-month old Wistar rats was dissected and biochemically compared to young adult muscle from 3-month old rats. Animals, which were kept at a standard light-dark cycle and fed *ad libitum*, were obtained from the Animal Facility of the Department of Physiology, Trinity College Dublin. Freshly dissected muscle specimens were quick-frozen in liquid nitrogen and ground into a fine powder using a mortar and pestle. Equal quantities of 100 mg wet weight of muscle were used for both young adult and senescent samples. The resulting tissue powder was placed into 1 ml of lysis buffer [7 M urea, 2 M thiourea, 20 mM Tris, 65 mM CHAPS, 100 mM DTT and 5% (v/v) pH 3.0-10 ampholytes]. To remove DNA, 2 $\mu$l of DNase-I (200 units) were added per 100 $\mu$l of lysis buffer. In order to prevent excess degradation of protein samples, the buffer was supplemented with a protease inhibitor cocktail containing 1 $\mu$M leupeptin, 1.4 $\mu$M pepstatin, 0.15 $\mu$M aprotinin, 0.5 mM soybean trypsin inhibitor, 0.2 mM prefabloc, 0.3 $\mu$M E-64 and 1 mM EDTA (31). Following 3 h of incubation at room temperature with vortexing every 10 min for 30 sec, the suspension was centrifuged for 20 min at 20,000 g. The lower layer of the supernatant, which contains the muscle protein fraction, was retained and samples were three times precipitated with acetone to remove any excess salts, lipids or nucleic acids (32). The final protein pellet was resuspended in 1 ml lysis buffer and its concentration determined using the Amersham 2-D Quant kit.

*2-D gel electrophoresis*. For isoelectric focusing, IPG strips were rehydrated for 12 h with rehydration buffer [7 M urea, 2 M thiourea, 20 mM Tris, 65 mM CHAPS, 100 mM DTT and 5% (v/v) pH 3.0-10 ampholytes; containing 0.05% (w/v) bromophenol blue as a tracking dye] in a re-swelling tray from Amersham Biosciences/GE Healthcare. After re-swelling, the IPG strips were loaded gel side up in an Amersham Ettan IPGphor manifold and covered with 108 ml of cover fluid. Five hundred $\mu$g of sample, either representing the total protein complement from young adult or old skeletal muscle,

was added by anodic cup loading to the strips and run on an Amersham IPGphor IEF system, employing the following running conditions: 30 V for 1 h, 100 V for 1 h, 500 V for 1 h, 1000 V for 1 h, 3000 V for 1 h, 6000 V 1 h, 8000 V for 3 h, 500 V for 4 h, and finally 8000 V for 3 h (33). Following isoelectric focusing, IPG strips were equilibrated twice for 30 min using 6 M urea, 30% (w/v) glycerol, 2% (w/v) sodium dodecyl sulfate, 100 mM Tris-HCl, pH 8.8, whereby the first incubation step was performed with the addition of 100 mM dithiothreitol and the second incubation step with 0.25 M iodoacetamide. The strips were then briefly washed in SDS running buffer and placed on top of 12.5% (w/v) resolving gels and kept in place using a 1% (w/v) agarose sealing gel. The gel electrophoretic separation of the skeletal muscle proteome in the second dimension was carried out by standard SDS-PAGE using an Amersham Ettan DALT-Twelve system (34). Gels were electrophoresed for 2 h at 30 V, followed by an 80-V step until the bromophenol blue dye front had just ran off the gel.

*Gel staining, image acquisition and 2-D image analysis.* Before staining with the fluorescent Deep Purple protein dye, 2-D gels were fixed using 7.5% (v/v) acetic acid and 10% (v/v) methanol. Gels were then washed for 30 min with a solution containing 35 mM sodium hydrogen carbonate and 300 mM sodium carbonate and incubated for 1 h in the dark with a 1:200 dilution of the Deep Purple stock solution (28-30). Following saturation with the protein dye, gels were destained twice for 15 min using 7.5% (v/v) acetic acid. Fluorescently labelled proteins were visualised using the Typhoon Trio variable mode imager from Amersham Biosciences/GE Healthcare at a scanning wavelength of λ=528 nm. The PMT values for gels analysed were between 500 V and 580 V, whereby scanning was performed at 100 $\mu$m resolution. 2-D gel images were cropped using ImageQuant TL software. In order to determine changes in protein levels, 2-D gel spot patterns from young adult versus old skeletal muscle preparations were compared across 10 gels using ImageMaster 2-D platinum (version 5) software. 2-D protein spots of interest that exhibited a 1.4-fold increase or decrease in expression were subsequently identified by MS analysis.

*Mass spectrometric protein identification.* In order to identify muscle proteins that showed a changed density between young adult and old *gastrocnemius* fibres, mass spectrometric PMF analysis (35) was employed using an Ettan MALDI-ToF Pro instrument from Amersham Biosciences. 2-D protein spots, which had been identified on fluorescently stained Deep Purple gels as being differentially expressed, were excised from Colloidal Coomassie Blue-stained pick gels that had been run in parallel in the above outlined Ettan DALT-Twelve gel electrophoretic separation system (32). Gel plugs were placed in 1.5 ml Eppendorf tubes which had been pre-siliconised with Sigmacote (Sigma Chemical Co.) and were then desalted, destained, washed, dried, digested and mixed with matrix by an optimized procedure recently described by our laboratory (31-34). The digestion solution contained 1 $\mu$g trypsin per 20 $\mu$l 50 mM $NH_4HCO_3$ and was applied for 1 h at 40˚C. The resulting peptide mixture was eluted onto the sample plate with an equal volume of matrix solution

containing 5 mg/ml α-cyano-4-hydroxycinnamic acid in 50% (v/v) acetonitrile/0.1% (v/v) trifluoroacetic acid. Recording of mass spectra using the MALDI-ToF method was carried out in the positive reflector mode, with an accelerating voltage of 20 kV and pulsed extraction on (focus mass of 2500). For convenient internal calibration, peptide products from trypsin autolysis activity at 221.104 m/z and 842.50 m/z were used. In addition, external peptides were also employed for calibration purposes. Peptidemix-1 from Laserbiolabs (Sophia-Antipolis, France) contains suitable peaks ranging from 1046.5 m/z to 2465.10 m/z. Analysis of the mass spectra was performed with Ettan MALDI evaluation software. For the identification of individual protein species, the ProFound database search engine for peptide mass fingerprints was used.

*Immunoblot analysis.* Proteins separated by 2-D gel electrophoresis, as described above in detail, were transferred to Immobilon NC-pure nitrocellulose membranes using a Transblot Cell from Bio-Rad Laboratories (Hemel Hempstead, Herts., UK) at 100 V for 70 min (36). To evaluate transfer efficiency, membrane sheets were reversibly stained with Ponceau-S Red. Removal of dye was achieved by several washes in 0.9% (w/v) NaCl, 50 mM sodium phosphate, pH 7.0. Blots were then blocked for 2 h in 5% (w/v) fat-free milk powder disolved in above phosphate-buffered saline and then incubated in suitably diluted primary antibody for 3 h, followed by two 10-min washes in blocking solution (37). Subsequently, immuno-decorated proteins were incubated with peroxidase-conjugated secondary antibody for 1 h, washed twice for 10 min in blocking solution and twice for 10 min in phosphate-buffered saline. Antibody-labelled 2-D protein spots were visualised by enhanced chemiluminescence using the Pierce Supersignal ECL kit (38). To compare the relative abundance of distinct muscle proteins in young adult versus senescent fibres, the densitometric analysis of immuno-decorated spots was carried out using a Molecular Dynamics 300S computing densitometer (Sunnyvale, CA, USA) with ImageMaster v5.0 software. Statistical evaluation of immuno-decoration was performed with Graphpad PRISM 5 software programme (Graphpad Software Inc., San Diego, CA).

**Results**

*2-D gel electrophoretic analysis of aging rat skeletal muscle.* In order to identify potential changes in the expression pattern of soluble skeletal muscle proteins during aging, total extracts from 3-month versus 30-month old rat *gastrocnemius* muscle were separated by standard 2-D gel electrophoresis. Isoelectric focusing in the first dimension was performed with a pH 3.0 to pH 10 gradient, which was followed by sodium dodecyl sulfate polyacrylamide gel electrophoresis covering a molecular mass range of ~10 kDa to 220 kDa in the second dimension. As illustrated by the two representative protein gels in Fig. 1, the fluorescent Deep Purple total protein stain revealed a relatively comparable overall 2-D protein spot pattern in young adult versus old muscle fibre preparations. The relative position of key skeletal muscle protein spots represented in this expression profile agreed with published results from international databanks (39-43) and our own previous studies on normal, dystrophic and transforming
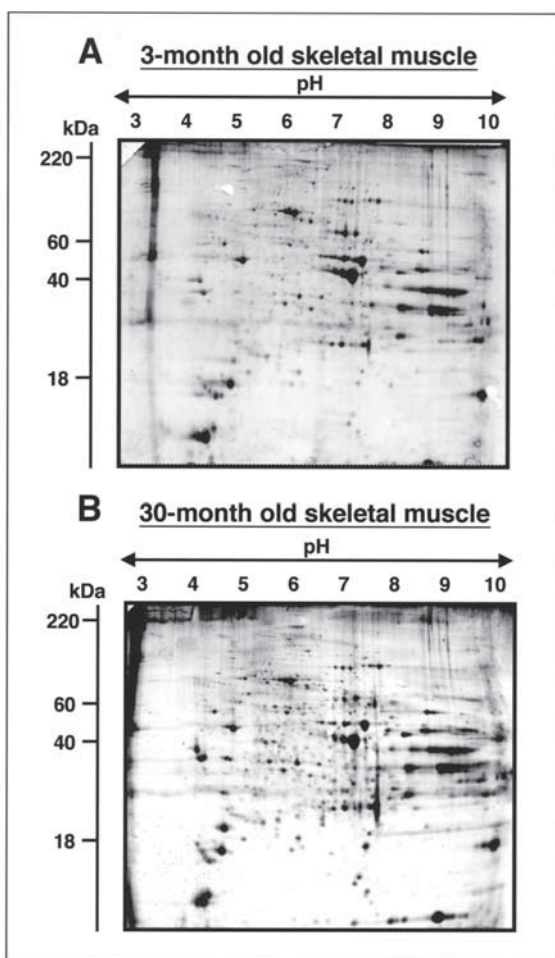
Figure 1. 2-D gel electrophoretic analysis of normal versus aged skeletal muscle extracts using fluorescent Deep Purple labelling. Shown are 2-D gel electrophoretically separated total *gastrocnemius* muscle extracts from young adult (A, 3-month old) and senescent (B, 30-month old) Wistar rats. The pH values of the first dimension gel system and molecular mass standards (in kDa) of the second dimension are indicated on the top and on the left of the panels, respectively.
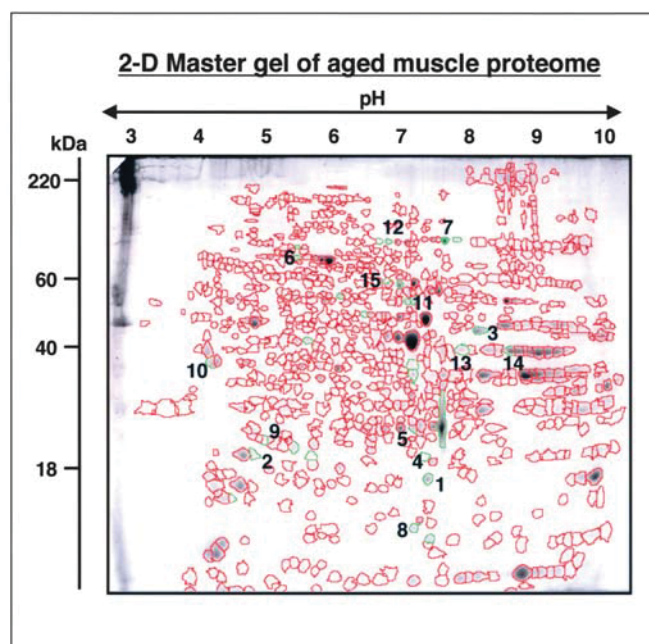


Figure 2. 2-D gel electrophoretic master map of the aged skeletal muscle proteome. Shown is a 2-D master gel of the aged *gastrocnemius* muscle proteome. Distinct 2-D protein spots are marked by red borders and muscle proteins that exhibited drastic changes in their abundance are indicated with green borders. Proteins with a drastically altered abundance, which have been identified by mass spectrometric PMF analysis, are numbered 1-15. See Table I for a detailed listing of density changes in αB-crystallin (pI 6.8; 20 kDa), myosin light chain 1 (pI 5; 21 kDa), phosphoglycerate kinase 1 (pI 8.3; 45 kDa), adenylate kinase 1 (pI 7.7; 22 kDa), triosephosphate isomerase Tpi1 (pI 7.1; 27 kDa), albumin (pI 6.1; 71 kDa) aconitase 2 (pI 8.2; 86 kDa), nucleoside-diphosphate kinase B (pI 6.9; 7.3 kDa), myosin light chain 3 (pI 5; 22 kDa), α-tropomyosin (pI 4.8; 34 kDa); creatine kinase (pI 8; 33 kDa); transferrin (pI 7; 79 kDa), aldolase A (pI 8.8; 39 kDa), and pyruvate kinase (pI 6.6; 58 kDa). The pH values of the first dimension gel system and molecular mass standards (in kDa) of the second dimension are indicated on the top and on the left of the panels, respectively.

muscle fibres (31-34). Thus, for the statistical evaluation of changes in individual protein spots, 2-D gel analysis software was employed, followed by the mass spectrometric PMF identification of candidate proteins.

*Differential protein expression pattern in young adult versus old rat skeletal muscle.* 2-D gel spot patterns were compared across 10 slab gels using the ImageMaster 2-D platinum software programme. Out of ~900 clearly separated 2-D protein spots that were recognized by Deep Purple staining, 30 spots were shown to be differentially expressed in 3-month versus 30-month old *gastrocnemius* muscle (Fig. 2). 2-D protein spots of interest that exhibited a 1.4-fold increase or decrease in expression were identified by MS methodology. PMF analysis using MALDI-ToF MS technology resulted in the identification of 14 distinct protein species. Changed muscle protein spots corresponded to αB-crystallin (pI 6.8; 20 kDa), myosin light chain 1 (pI 5; 21 kDa), phosphoglycerate kinase 1 (pI 8.3; 45 kDa), adenylate kinase 1 (pI 7.7; 22 kDa), Tpi1 protein (pI 7.1; 27 kDa), albumin (pI 6.1; 71 kDa) aconitase 2 (pI 8.2; 86 kDa), nucleoside-diphosphate kinase B (pI 6.9; 17.3 kDa), myosin light chain 3 (pI 5; 22 kDa),

α-tropomyosin (pI 4.8; 34 kDa); creatine kinase (pI 8; 33 kDa); transferrin (pI 7; 79 kDa), aldolase A (pI 8.8; 39 kDa), and pyruvate kinase (pI 6.6; 58 kDa). Table I summarises the information gained from the proteomic profiling of aged skeletal muscle fibres. The table gives detailed information on the spot number of proteins with a changed density, so that they can be correlated to the numbering in the 2-D master gel of the aged skeletal muscle proteome shown in Fig. 2. Table I lists the percentage coverage of the PMF-identified peptide fragments with respect to the total primary muscle protein sequence, the isoelectric point of the identified protein, its apparent molecular mass and the fold change in density.

As can be seen in Table I, the small heat shock protein αB-crystallin (spot 1), the contractile element myosin light chain isoform MLC-1 (spot 2) and the enzyme phosphoglycerate kinase 1 (spot 3) exhibited a drastic increase in abundance. The enzyme adenylate kinase (spot 4), crucial for nucleotide metabolism, and the triosephosphate isomerase isoform Tpi1 (spot 5) showed both an ~1.5-fold increase in expression. Importantly, the extracellular fatty acid transport protein albumin (spot 6) was found to be increased, suggesting a shift to more aerobic-oxidative metabolism in aged fibres. In agreement, the mitochondrial citric acid cycle marker aconitase-2 represented by 2-D spot 7 was shown to be

Table I. List of identified protein species that exhibit a drastic change in expression in 3-month versus 30-month old rat *gastrocnemius* muscle.

| Spot no. | Name of identified protein | Protein accession no. | Sequence coverage (%) | pI | Molecular mass (kDa) | Fold change +/- |
|---|---|---|---|---|---|---|
| 1 | αB-crystallin | gil30387800l | 49.0 | 6.8 | 20.15 | 2.45 |
| 2 | Myosin light chain 1 | gil127131l | 54.0 | 5 | 20.66 | 1.91 |
| 3 | Phosphoglycerate kinase 1 | gil38649310l | 33.6 | 8.3 | 44.92 | 1.59 |
| 4 | Adenylate kinase 1 | gil23831184l | 43.8 | 7.7 | 21.64 | 1.56 |
| 5 | Triosephosphate isomerase Tpi1 | gil38512111l | 23.8 | 7.1 | 27.21 | 1.54 |
| 6 | Albumin | gil55391508l | 17.0 | 6.1 | 70.74 | 1.47 |
| 7 | Aconitase ACO2 | gil38541404l | 27.6 | 8.2 | 86.16 | 1.46 |
| 8 | Nucleoside-diphosphate kinase NDK-B | gil127984l | 49.0 | 6.9 | 17.3 | 1.40 |
| 9 | Myosin light chain 3 | gil6981240l | 60.0 | 5 | 22.14 | -1.39 |
| 10 | α-tropomyosin | gil207352l | 44.6 | 4.8 | 33.82 | -1.52 |
| 11 | Creatine kinase | gil203480l | 23.0 | 8 | 33.43 | -1.55 |
| 12 | Transferrin | gil6175089l | 6.6 | 7 | 78.57 | -1.66 |
| 13 | Creatine kinase | gil203480l | 34.0 | 8 | 33.43 | -1.91 |
| 14 | Aldolase A | gil6978487l | 30.0 | 8.8 | 39.33 | -1.99 |
| 15 | Pyruvate kinase | gil16757994l | 18.0 | 6.6 | 57.8 | -2.62 |

increased in its expression. However, immuno-decoration of the entire aconitase complement, as described below, did not confirm that all aconitase isoforms are affected in the same way during fibre aging. Nucleoside-diphosphate kinase isoform NDK-B (spot 8) exhibited an increased expression. In contrast, the contractile elements myosin light chain MLC-3 (spot 9) and α-tropomyosin (spot 10) showed a decreased density in senescent fibres. The glycolytic enzymes aldolase A (spot 14) and pyruvate kinase (spot 15) exhibited a drastic 2- and 2.6-fold decrease, respectively. In addition, transferrin (spot 12) and creatine kinase (spots 11 and 13) showed an apparent down-regulation in senescent muscle. Several un-identified proteins exhibited an increased or decreased density in aged fibres (Fig. 2), but MS analysis of its peptide fragments failed to give reliable data for proper identification (data not shown). A Deep Purple-labelled 2-D spot at position pI 6.9/29.4 kDa was identified by PMF analysis as the muscle isoform CA3 of carbonic anhydrase. Densitometric scanning revealed a 4.5-fold increase, which however was not confirmed by immunoblotting as shown below. Since the CA3-containing spot was part of a larger elongated 2-D spot cluster, which included other abundant muscle proteins, the densitometric analysis lead to a false positive. This finding illustrates the importance of confirming the results from proteomic profiling studies based on MALDI-ToF technology, using other bio-chemical or cell biological methods, such as immunoblotting or immunofluorescence microscopy.

*Immunoblot analysis of biomarkers of sarcopenia of old age.* To document the reliability of the comparative densitometric analysis of 2-D spot patterns following staining with the fluorescent dye Deep Purple and in order to confirm the protein identification via MS-based MALDI-ToF proteomics,
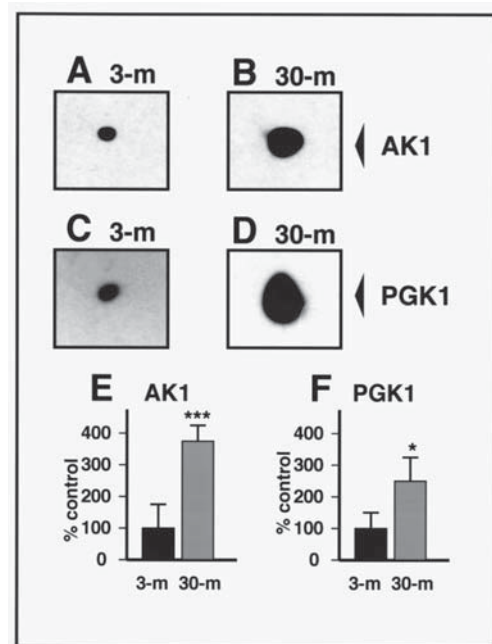


Figure 3. 2-D immunoblot analysis of adenylate kinase and phospho-glycerate kinase in aged skeletal muscle. Shown is the immuno-decoration of nitrocellulose replicas of 2-D gels, as shown in Fig. 1, representing total *gastrocnemius* muscle extracts from young adult (A and C, 3-month old) and senescent (B and D, 30-month old) Wistar rats. Antibodies were directed against adenylate kinase (A and B, AK1), and phosphoglycerate kinase (C and D, PGK1). The comparative immunoblotting with 3-month versus 30-month old muscle preparations was statistically evaluated using an unpaired Student's t-test (n=5; *p<0.01; ***p<0.001) and is graphically shown in panels (E) and (F).

we picked several representative proteins of the group of up- and down-regulated muscle proteins for 2-D immunoblotting studies. As illustrated in Fig. 3A-D, the increase in adenylate
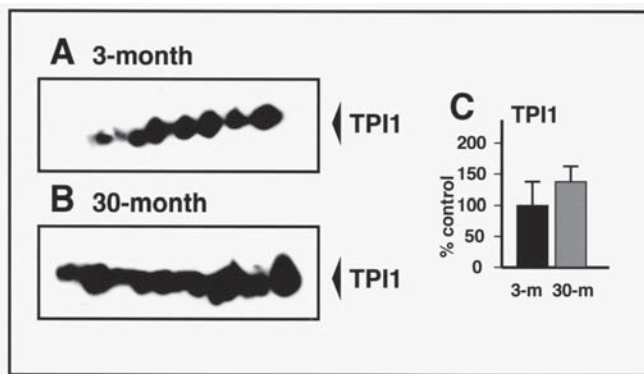
Figure 4. 2-D immunoblot analysis of triosephosphate isomerase in aged skeletal muscle. Shown is the immuno-decoration of nitrocellulose replicas of 2-D gels, as shown in Fig. 1, representing total *gastrocnemius* muscle extracts from young adult (A, 3-month old) and senescent (B, 30-month old) Wistar rats. Antibodies were directed against triosephosphate isomerase (A and B, TPI1). The comparative immunoblotting with 3-month versus 30-month old muscle preparations was statistically evaluated using an unpaired Student's t-test (n=5; no significant difference) and is graphically shown in panel (C).



Figure 6. 2-D immunoblot analysis of transferrin, aldolase and carbonic anhydrase in aged skeletal muscle. Shown is the immuno-decoration of nitrocellulose replicas of 2-D gels, as shown in Fig. 1, representing total *gastrocnemius* muscle extracts from young adult (A, C and E, 3-month old) and senescent (B, D and F, 30-month old) Wistar rats. Antibodies were directed against transferrin (A and B, TF), aldolase (C and D, ALD-A), and the muscle-specific carbonic anhydrase (E and F, CA3). The comparative immunoblotting with 3-month versus 30-month old muscle preparations was statistically evaluated using an unpaired Student's t-test (n=5; $^*p<0.05$; $^{**}p<0.01$) and is graphically shown in panels (G) to (I).
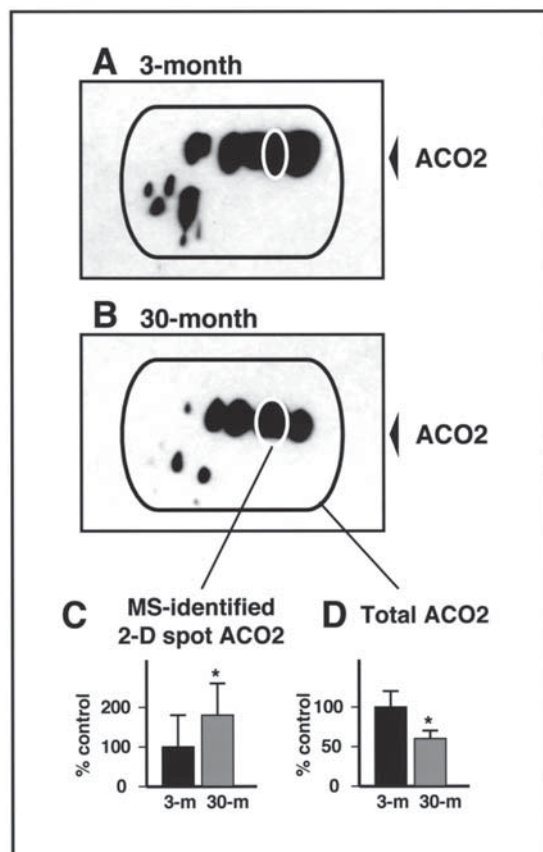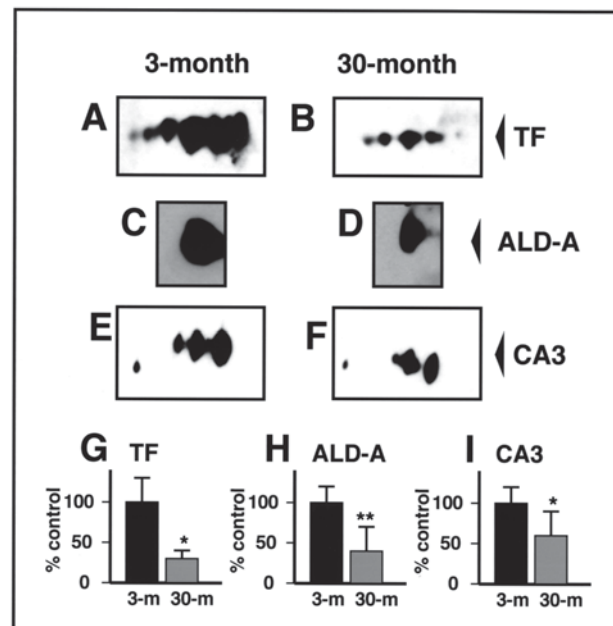


Figure 5. 2-D immunoblot analysis of aconitase in aged skeletal muscle. Shown is the immuno-decoration of nitrocellulose replicas of 2-D gels, as shown in Fig. 1, representing total *gastrocnemius* muscle extracts from young adult (A, 3-month old) and senescent (B, 30-month old) Wistar rats. Antibodies were directed against aconitase (A and B, ACO2). White circles mark the MS-identified aconitase 2-D spot (see Table I) and the black border surrounds the total cohort of ACO2-labelled protein spots. The comparative immunoblotting with 3-month versus 30-month old muscle preparations was statistically evaluated using an unpaired Student's t-test (n=5; $^*p<0.05$) and is graphically shown in panels (C) and (D).

kinase and phosphoglycerate kinase in aged fibres was clearly confirmed by immuno-decoration with highly specific anti-

bodies. The statistically significant differences in expression levels (Fig. 3E and F) correlated relatively well with the proteomic survey listed in Table I. While single protein species were recognized in the case of the AK1 and PGK1 isoforms, antibody labelling of triosephosphate isomerase revealed a cohort of eight individual 2-D spots representing this essential metabolic enzyme (Fig. 4A and B). Although the statistical analysis of Western blotting showed no significant difference in the abundance of these proteins between young adult and senescent muscle fibres, the analysis indicates a trend towards an increased expression of the TPI1 isoform in aged muscle (Fig. 4C). The immunoblotting of mitochondrial aconitase isoform ACO2 gave an interesting result, since it confirmed the increase of a distinct 2-D spot representing this enzyme, but an overall decrease of the entire immuno-decorated aconitase complement in aged skeletal muscle (Fig. 5A and B). Hence, the MS-identified ACO2 spot with a higher density does not seem to be representative for the total cohort of aconitase species in skeletal muscle (Fig. 5C and D). The decreased abundance of transferrin and aldolase was confirmed by immunoblotting (Fig. 6A-D) and the statistical analysis (Fig. 6G and H) correlated relatively well with the findings from the proteomic profiling study summarized in Table I. Antibody labelling of the muscle-specific CA3 isoform of carbonic anhydrase showed a decreased abundance of this enzyme in aged fibres (Fig. 6E, F and I), therefore demonstrating that the MS-identified CA3-spot included other more abundant muscle proteins besides carbonic anhydrase. It is encouraging that antibody staining confirmed the identification

of individual muscle proteins and that this technique was able to clarify their change in expression levels during aging. This demonstrates the reliability of MS protein identification methodology and shows that the overall rate of correct evaluation of 2-D spot density by densitometric analysis of Deep Purpled stained 2-D gels is very high.

## Discussion

The pathophysiology of sarcopenia is characterised by a significant reduction in overall skeletal muscle mass, a decrease in fibre strength and increased fatigability (7,8). Sarcopenia appears to occur in most humans to some degree as a consequence of aging, but may develop into a serious neuromuscular pathology in senescent individuals (3). Severe forms of sarcopenia can be accelerated by a variety of factors including inactivity, poor nutrition and chronic illness (2). It is estimated that from the fourth decade on, approximately five percent of skeletal muscle mass is lost per decade (1). In this respect, the research outlined in this project will attempt to systematically determine abnormal protein expression patterns in senescent muscle tissue. This might unearth new ways to treat muscular weakness in the aging population (22). The proteomic profiling of an animal model of sarcopenia, 30-month old *gastrocnemius* muscles from Wistar rats, has clearly shown a severely disturbed protein expression pattern in senescent fibres as compared to young adult tissue. This has included proteins involved in stress response, the contractile apparatus and metabolic regulation. These protein species can now be taken as a starting point for in-depth biochemical, cell biological and physiological characterization of aged muscle fibres. 2-D gel electrophoresis is a highly reproducible technique (44) and proteomic surveys usually exhibit very few false positive or negative results (45). Hence, the findings from proteomic profiling exercises can give reliable trends about biological changes in pathological tissues (23) and can be exploited in the design of future clinical studies (24).

The cohort of biomarkers identified by the animal model proteomic survey described here demonstrates a distinct up-regulation of cellular stress elements. The drastic increase of the small heat shock protein αB-crystallin in senescent skeletal muscle suggests that age-dependent alterations in cytoskeletal filaments are counteracted by the increase in distinct chaperones. Small stress proteins are relatively abundant in muscle tissues (46) and the chaperone activity of the α-crystallin subfamily of proteins was shown to be involved in the modulation of intermediate filament assembly (47). Continuous contractile activity has a considerable effect on the expression levels of αB-crystallin (48,49) making the finding presented here an interesting observation with respect to the mechanisms underlying fibre modifications during aging. Since the aggregation of denatured muscle proteins may be detrimental to the cellular homeostasis of aged fibres, the increased presence of small heat shock proteins is probably involved in reversing the age-related damage to skeletal muscles. As reviewed by Nishimura and Sharp (50), heat shock proteins play a central role in many neuromuscular diseases. This includes x-linked Duchenne muscular dystrophy (51). It was recently shown that the small heat shock protein cvHSP

is greatly increased in its abundance in the dystrophin-deficient diaphragm (32). Possibly, the muscle-specific family of low-molecular-mass stress proteins represents an important new class of diagnostic markers and/or therapeutic targets in common muscle disorders.

The disturbed expression pattern of tropomyosin and myosin light chains (52), as described here, agrees with previous proteomic studies on muscle aging (27,53). As shown by numerous studies, the integrity of the aged motor unit is severely impaired in aged fibres (4,5). Changes in fibre innervation has a profound effect on the mechanical properties of senescent fibres (18). Interestingly, denervated muscles and aged fibre populations show many similarities, suggesting that sarcopenia might be at least partially due to impaired neuronal transmission (19). Since the degree of neuromuscular activity dictates gene expression patterns in the multi-nucleated muscle fibres belonging to a motor unit (54), pathophysiological alterations in the innervating motor neuron system will negatively affect muscle protein expression levels. Although a metabolic shift towards more aerobic-oxidative metabolism and slower switch characteristics are evident in older skeletal muscles (3,7,8), the molecular alterations within the contractile apparatus are extremely complex and do not necessarily agree with a predominant transformation to slower fibres (53). The proteomics findings shown here suggest changes in glycolytic enzymes and key elements of the citric acid cycle (55). Individual proteins belonging to the same major metabolic pathway may be affected in a differential way. While the expression of phosphoglycerate kinase and triosephosphate isomerase were shown to be increased, pyruvate kinase and aldolase levels were decreased. Since phosphoglycerate kinase and pyruvate kinase represent two glycolytic enzymes that are both involved in separate key ATP-generating reactions, these results suggest complex metabolic alterations in aged fibres. Additional more comprehensive investigations into the entire cohort of enzymes responsible for glucose metabolism are necessary to determine the exact fate of glycolytic enzymes during skeletal muscle aging.

The recent proteomic profiling of transforming fibres has shown a clear down-regulation of glycolytic enzymes and a concomitant increase in the mitochondrial protein machinery during the fast-to-slow transition process (33). In comparison, the biochemical changes occurring in aging fibres appear to be more complex and do not appear to reflect just fibre transformation, but also muscular atrophy. Since the MS identification of an up-regulated mitochondrial aconitase isoform indicated a shift to a higher degree of aerobic-oxidative metabolism in aged fibres, but immunoblotting did not confirm an overall increase in the entire aconitase complement, the transition to more oxidative metabolism seems to be extremely complex. Decreased aconitase levels agreed with a previous study which suggests that oxidative damage during aging targets mitochondrial aconitase (56). Interestingly, previous metabolic studies comparing chronic low-frequency stimulated young versus aged fibres suggest that both muscle types respond in a similar way to sustained neuromuscular activity (57,58). Therefore, the age-induced changes in glycolytic and mitochondrial enzymes might be a consequence of altered innervation patterns and not a

primary pathological insult within the skeletal muscle fibres themselves.

The increased density of the extracellular fatty acid-transporter albumin, a crucial multi-functional muscle protein with respect to protein metabolism, fatty acid oxidation and osmotic fibre balance (59), agrees however with a shift towards oxidative bioenergetics in older muscle fibres. Both, the intracellular fatty acid binding protein FABP and its external counterpart albumin, in combination with myoglobin levels, are believed to be limiting factors of oxidative muscle metabolism. Therefore, the increased albumin density in the aged skeletal muscle proteome indicates decrease anaerobic metabolism in sarcopenia of old age. The enzymes adenylate kinase, nucleoside diphosphate kinase and creatine kinase, differentially affected in aged fibres, provide a major nucleotide pathway in skeletal muscle (60,61). Alterations in their expression profile suggest an abnormal regulation of nucleotide ratios in aged fibres. Another potentially important result with respect to muscle metabolism is the decreased expression level of transferrin, a crucial metal ion-transporting protein. Reduced transferrin levels may trigger pathological free serum iron levels rendering individuals more susceptible to infection by iron-dependent microorganisms (62).

In conclusion, although the biochemical and cellular mechanisms that underlie sarcopenia of old age are only beginning to be elucidated, MS-based proteomic studies into the pathophysiological mechanisms of muscle aging might produce novel cohorts of disease markers. Such detailed biochemical knowledge can then be used to evaluate which combination of neurogenic and myogenic factors determines the destructive pathways leading to sarcopenia. Since proper neuronal activity is a crucial factor for the maintenance of skeletal muscle mass and strength, eliminating denervation of aged fibres will probably be one of the most important steps in the clinical treatment of sarcopenia. The alterations in the expression levels of distinct classes of skeletal muscle proteins presented in this report could be used to design more elaborate biochemical surveys of age-induced fibre degeneration. For example, fluorescence difference in-gel electrophoresis (63) is several times more sensitive than conventional proteomics (64,65). The recent difference in-gel electrophoretic analysis of dystrophic muscle fibres exhibited a 7-fold increase in its protein detection rate as compared to conventional protein staining techniques (32). Hence, the application of novel fluorescent techniques for the detection of differential protein expression patterns in pathological specimens may lead to improved diagnostic procedures and/or new treatment strategies for common neuromuscular disorders and thus improve the standard of living of a large portion of society.

## Acknowledgements

## References

1. Melton LJ III, Khosla S, Crowson CS, O'Connor MK, O'Fallon WM and Riggs BL: Epidemiology of sarcopenia. J Am Geriatr Soc 48: 625-630, 2000.
2. Morley JE, Baumgartner RN, Roubenoff R, Mayer J and Nair KS: Sarcopenia. J Lab Clin Med 137: 231-243, 2001.
3. Greenlund LJS and Nair KS: Sarcopenia - consequences, mechanisms, and potential therapies. Mech Ageing Dev 124: 287-299, 2003.
4. Larsson L and Ansved T: Effects of ageing on the motor unit. Prog Neurobiol 45: 397-458, 1995.
5. Larsson L: The age-related motor disability: underlying mechanisms in skeletal muscle at the motor unit, cellular and molecular level. Acta Physiol Scand 163: S27-S29, 1998.
6. Vandervoort AA and Symons TB: Functional and metabolic consequences of sarcopenia. Can J Appl Physiol 26: 90-101, 2001.
7. Navarro A, Lopez-Cepero JM and Sanchez del Pino MJ: Skeletal muscle ageing. Front Biosci 6: 26-44, 2001.
8. Carmeli E, Coleman R and Reznick AZ: The biochemistry of aging muscle. Exp Gerontol 37: 477-489, 2002.
9. Squier TS and Bigelow DJ: Protein oxidation and age-dependent alterations in calcium homeostasis. Front Biosci 5: 504-526, 2000.
10. Bua EA, McKiernan SH, Wanagat J, McKenzie D and Aiken JM: Mitochondrial abnormalities are more frequent in muscles undergoing sarcopenia. J Appl Physiol 92: 2617-2624, 2002.
11. Dirks A and Leeuwenburgh C: Apoptosis in skeletal muscle with aging. Am J Physiol 282: R519-R527, 2002.
12. Roberts SB: Effects of aging on energy requirements and the control of food intake in men. J Gerontol 50A: 101-106, 1995.
13. Degens H: Age-related changes in the microcirculation of skeletal muscle. Adv Exp Med Biol 454: 343-348, 1998.
14. Balagopal P, Rooyackers OE, Adey DB, Ades PA and Nair KS: Effects of aging on *in vivo* synthesis of skeletal muscle myosin heavy-chain and sarcoplasmic protein in humans. Am J Physiol 273: E790-E800, 1997.
15. Renault V, Thornell LE, Eriksson PO, Butler-Browne G and Mouly V: Regenerative potential of human skeletal muscle during aging. Aging Cell 1: 132-139, 2002.
16. Ryan M, Carlson BM and Ohlendieck K: Oligomeric status of the dihydropyridine receptor in aged skeletal muscle. Mol Cell Biol Res Commun 4: 224-229, 2001.
17. Ryan M and Ohlendieck K: Excitation-contraction uncoupling and sarcopenia. Bas Appl Myol 14: 141-154, 2004.
18. Luff AR: Age-associated changes in the innervation of muscle fibres and changes in the mechanical properties of motor units. Ann NY Acad Sci 854: 92-101, 1998.
19. Carlson BM: Denervation and the aging of skeletal muscle. Bas Appl Myol 14: 135-140, 2004.
20. De Hoog CL and Mann M: Proteomics. Annu Rev Genomics Hum Genet 5: 267-293, 2004.
21. Toda T: Proteome and proteomics for the research on protein alterations in aging. Ann NY Acad Sci 928: 71-78, 2001.
22. Schoneich C: Proteomics in gerontological research. Exp Gerontol 38: 473-481, 2003.
23. Doran P, Donoghue P, O'Connell K, Gannon J and Ohlendieck K: Proteomic profiling of pathological and aged skeletal muscle fibres by peptide mass fingerprinting (Review). Int J Mol Med 19: 547-564, 2007.
24. Doran P, Gannon J, O'Connell K and Ohlendieck K: Proteomic profiling of animal models mimicking skeletal muscle disorders. Proteomics Clin Appl (In press).
25. Kanski J, Alterman MA and Schoneich C: Proteomic identification of age-dependent protein nitration in rat skeletal muscle. Free Radic Biol Med 35: 1229-1239, 2003.
26. Kanski J, Hong SJ and Schoneich C: Proteomic analysis of protein nitration in aging skeletal muscle and identification of nitrotyrosine-containing sequences *in vivo* by nanoelectrospray ionization tandem mass spectrometry. J Biol Chem 280: 24261-24266, 2005.
27. Piec I, Listrat A, Alliot J, Chambon C, Taylor RG and Bechet D: Differential proteome analysis of aging in rat skeletal muscle. FASEB J 19: 1143-1145, 2005.
28. Bell PJL and Karuso P: Epicocconone, a novel fluorescent compound from the fungus *Epicoccum nigrum*. J Am Chem Soc 125: 9304-9305, 2003.
29. Coghlan DR, Mackintosh JA and Karuso P: Mechanism of reversible fluorescent staining of protein with epicocconone. Org Lett 7: 2401-2404, 2005.

30. Mackintosh JA, Choi HY, Bae SH, Veal DA, Bell PJ, Ferrari BC, Dyk DDV, Verrills NM, Paik YK and Karuso P: A fluorescent natural product for ultra sensitive detection of proteins in one-dimensional and two-dimensional gel electrophoresis. Proteomics 3: 2273-2288, 2003.

31. Doran P, Dowling P, Lohan J, McDonnell K, Poetsch S and Ohlendieck K: Subproteomics analysis of $Ca^{2+}$-binding proteins demonstrates decreased calsequestrin expression in dystrophic mouse skeletal muscle. Eur J Biochem 271: 3943-3952, 2004.

32. Doran P, Martin G, Dowling P, Jockusch H and Ohlendieck K: Proteome analysis of the dystrophin-deficient MDX diaphragm reveals a drastic increase in the heat shock protein cvHSP. Proteomics 6: 4610-4621, 2006.

33. Donoghue P, Doran P, Dowling P and Ohlendieck K: Differential expression of the fast skeletal muscle proteome following chronic low-frequency stimulation. Biochim Biophys Acta 1752: 166-176, 2005.

34. Doran P, Dowling P, Donoghue P, Buffini M and Ohlendieck K: Reduced expression of regucalcin in young and aged mdx diaphragm indicates abnormal cytosolic calcium handling in dystrophin-deficient muscle. Biochim Biophys Acta 1764: 773-785, 2006.

35. Webster J and Oxley D: Peptide mass fingerprinting: protein identification using MALDI-TOF mass spectrometry. Methods Mol Biol 310: 227-240, 2005.

36. Towbin H, Staehelin T and Gordon J: Immunoblotting in the clinical laboratory. J Clin Chem Clin Biochem 27: 495-501, 1989.

37. Culligan K, Banville N, Dowling P and Ohlendieck K: Drastic reduction of calsequestrin-like proteins and impaired calcium binding in dystrophic mdx muscle. J Appl Physiol 92: 435-445, 2002.

38. Dowling P, Doran P and Ohlendieck K: Drastic reduction of sarcalumenin in Dp427 (dystrophin of 427 kDa)-deficient fibres indicates that abnormal calcium handling plays a key role in muscular dystrophy. Biochem J 379: 479-488, 2004.

39. Isfort RJ: Proteomic analysis of striated muscle. J Chromatogr B 771: 155-165, 2002.

40. Sanchez JC, Chiappe D, Converset V, Hoogland C, Binz PA, Paesano S, Appel RD, Wang S, Sennitt M, Nolan A, Cawthorne MA and Hochstrasser DF: The mouse SWISS-2D PAGE database: a tool for proteomics study of diabetes and obesity. Proteomics 1: 136-163, 2001.

41. Yan JX, Harry RA, Wait R, Welson SY, Emery PW, Preedy V and Dunn MJ: Separation and identification of rat skeletal muscle proteins using two-dimensional gel electrophoresis and mass spectrometry. Proteomics 1: 424-434, 2001.

42. Okumura N, Hashida-Okumura A, Kita K, Matsubae M, Matsubara T, Takao T and Nagai K: Proteomic analysis of slow- and fast-twitch skeletal muscles. Proteomics 5: 2896-2906, 2006.

43. Gelfi C, Vigano A, De Palma S, Ripamonti M, Begum S, Cerretelli P and Wait R: 2-D protein maps of rat gastrocnemius and soleus muscles: a tool for muscle plasticity assessment. Proteomics 6: 321-340, 2006.

44. Gorg A, Weiss W and Dunn MJ: Current two-dimensional electrophoresis technology for proteomics. Proteomics 4: 3665-3685, 2004.

45. Domon B and Aebersold R: Mass spectrometry and protein analysis. Science 312: 212-217, 2006.

46. De Jong WW, Leunissen JA and Voorter CE: Evolution of the alpha-crystallin/small heat shock protein family. Mol Biol Evol 10: 103-126, 1993.

47. Nicholl ID and Quinlan RA: Chaperone activity of alpha-crystallins modulates intermediate filament assembly. EMBO J 13: 945-953, 1994.

48. Neufer PD and Benjamin IJ: Differential expression of B-crystallin and Hsp27 in skeletal muscle during continuous contractile activity. Relationship to myogenic regulatory factors. J Biol Chem 271: 24089-24095, 1996.

49. Neufer PD, Ordway GA and Williams RS: Transient regulation of c-fos, alpha B-crystallin, and hsp70 in muscle during recovery from contractile activity. Am J Physiol 274: C341-C346, 1998.

50. Nishimura RN and Sharp FR: Heat shock proteins and neuro-muscular disease. Muscle Nerve 32: 693-709, 2005.

51. Bornman L, Polla BS, Lotz BP and Gericke GS: Expression of heat-shock/stress proteins in Duchenne muscular dystrophy. Muscle Nerve 18: 23-31, 1995.

52. Gonzalez B, Negredo P, Hernando R and Manso R: Protein variants of skeletal muscle regulatory myosin light chain isoforms: prevalence in mammals, generation and transitions during muscle remodeling. Pflugers Arch 443: 377-386, 2002.

53. Gelfi C, Vigano A, Ripamonti M, Pontoglio A, Begum S, Pellegrino MA, Grassi B, Bottinelli R, Wait R and Cerretelli P: The human muscle proteome in aging. J Proteome Res 5: 1344-1353, 2006.

54. Pette D and Staron RS: Cellular and molecular diversities of mammalian skeletal muscle fibers. Rev Physiol Biochem Pharmacol 116: 1-76, 1990.

55. Erlandsen H, Abola EE and Stevens RC: Combining structural genomics and enzymology: completing the picture in metabolic pathways and enzyme active sites. Curr Opin Struct Biol 10: 719-730, 2000.

56. Yan LJ, Levine RL and Sohal RS: Oxidative damage during aging targets mitochondrial aconitase. Proc Natl Acad Sci USA 94: 11168-11172, 1997.

57. Skorjanc D, Traub I and Pette D: Identical responses of fast muscle to sustained activity by low-frequency-stimulation in young and aging rats. J Appl Physiol 85: 437-441, 1998.

58. Pette D and Skorjanc D: Adaptive potentials of skeletal muscle in young and aging rats. Int J Sport Nutr Exerc Metab 11: S3-S8, 2001.

59. Heilig A and Pette D: Albumin in rabbit skeletal muscle. Origin, distribution and regulation by contractile activity. Eur J Biochem 171: 503-508, 1988.

60. Dzeja PP, Bortolon R, Perez-Terzic C, Holmuhamedov EL and Terzic A: Energetic communication between mitochondria and nucleus directed by catalyzed phosphotransfer. Proc Natl Acad Sci USA 99: 10156-10161, 2002.

61. Benz R, Kottke M and Brdiczka D: The cationically selective state of the mitochondrial outer membrane pore: a study with intact mitochondria and reconstituted mitochondrial porin. Biochim Biophys Acta 1022: 311-318, 1990.

62. Beard JL: Iron biology in immune function, muscle metabolism and neuronal functioning. J Nutr 131: 568S-579S, 2001.

63. Unlu M: Difference gel electrophoresis. Biochem Soc Trans 27: 547-549, 1999.

64. Tonge R, Shaw J, Middleton B, Rowlinson R, Rayner S, Young J, Pognan F, Hawkins E, Currie I and Davison M: Validation and development of fluorescence two-dimensional differential gel electrophoresis proteomics technology. Proteomics 1: 377-396, 2001.

65. Marouga R, David S and Hawkins E: The development of the DIGE system: 2D fluorescence difference gel analysis technology. Anal Bioanal Chem 382: 669-678, 2005.